

Replication stress induces 53BP1-containing OPT domains in G1 cells

Jeanine A. Harrigan,¹ Rimma Belotserkovskaya,¹ Julia Coates,¹ Daniela S. Dimitrova,² Sophie E. Polo,¹ Charles R. Bradshaw,¹ Peter Fraser,² and Stephen P. Jackson¹

¹The Gurdon Institute, University of Cambridge, Cambridge CB2 1QN, England, UK

²Laboratory of Chromatin and Gene Expression, Babraham Institute, Babraham Research Campus, Cambridge CB22 3AT, England, UK

Chromosomal deletions and rearrangements in tumors are often associated with common fragile sites, which are specific genomic loci prone to gaps and breaks in metaphase chromosomes. Common fragile sites appear to arise through incomplete DNA replication because they are induced after partial replication inhibition by agents such as aphidicolin. Here, we show that in G1 cells, large nuclear bodies arise that contain p53 binding protein 1 (53BP1), phosphorylated H2AX (γ H2AX), and mediator of DNA damage checkpoint 1 (MDC1), as well as components of previously characterized

OPT (Oct-1, PTF, transcription) domains. Notably, we find that incubating cells with low aphidicolin doses increases the incidence and number of 53BP1-OPT domains in G1 cells, and by chromatin immunoprecipitation and massively parallel sequencing analysis of γ H2AX, we demonstrate that OPT domains are enriched at common fragile sites. These findings invoke a model wherein incomplete DNA synthesis during S phase leads to a DNA damage response and formation of 53BP1-OPT domains in the subsequent G1.

Introduction

Maintaining the integrity of DNA during transactions such as transcription, replication, and repair is critical for preventing chromosomal mutations, deletions, and rearrangements that may ultimately lead to cancer. Replication of the human genome is a highly complex process that enables the effective and accurate duplication of genetic information. Most crucially, DNA replication is tightly monitored to ensure that the genome is replicated just once per cell cycle and that replication is complete before mitosis begins (Branzei and Foiani, 2010). Similarly, cellular responses to DNA double-strand breaks (DSBs) are highly coordinated and involve the sensing of damaged DNA together with signaling to DNA repair, cell-cycle checkpoint, and apoptotic machineries (Ciccia and Elledge, 2010).

The eukaryotic genome contains numerous natural impediments to replication, including unusual DNA structures,

DNA-binding proteins, highly transcribed DNA sequences, and slow replication zones (Branzei and Foiani, 2010). Chromosomal fragile sites, which are classified as either rare or common, are specific genomic loci that display gaps or breaks on metaphase chromosomes after partial inhibition of DNA synthesis (Durkin and Glover, 2007). The majority of common fragile sites are induced by treatment with low doses of aphidicolin (APH), an inhibitor of replicative polymerases, which suggests that they arise as a consequence of replication stress (Glover et al., 1984). Common fragile sites have received particular attention in recent years because they are sites of frequent deletions and other chromosome rearrangements in tumor cells (Durkin and Glover, 2007).

p53 binding protein 1 (53BP1) is an important component of the DNA damage response (DDR) that localizes to microscopically visible foci at DSB sites (Schultz et al., 2000). Animals or cells lacking 53BP1 are hypersensitive to ionizing radiation, and display DNA damage checkpoint defects and impaired DNA repair (Ward et al., 2003). 53BP1 also plays important roles

Correspondence to Stephen P. Jackson: s.jackson@gurdon.cam.ac.uk

Abbreviations used in this paper: 53BP1, p53 binding protein 1; APH, aphidicolin; ATM, ataxia telangiectasia mutated; BLM, Bloom syndrome helicase; Cyc A, Cyclin A; DDR, DNA damage response; DSB, double-strand break; EdU, 5-ethynyl-2'-deoxyuridine; FA, formaldehyde; FlU, 5-fluorouridine; hTERT, human telomerase reverse transcriptase; HU, hydroxyurea; MDC1, mediator of DNA damage checkpoint 1; MEF, mouse embryonic fibroblast; OPT, Oct-1, PTF, transcription; Pol II, RNA polymerase II; PSQF, penicillin, streptomycin, glutamine, and fungazone; ssDNA, single-stranded DNA.

© 2011 Harrigan et al. This article is distributed under the terms of an Attribution-Noncommercial-Share Alike-No Mirror Sites license for the first six months after the publication date [see <http://www.rupress.org/terms>]. After six months it is available under a Creative Commons License [Attribution-Noncommercial-Share Alike 3.0 Unported license, as described at <http://creativecommons.org/licenses/by-nc-sa/3.0/>].

in class switch recombination at immunoglobulin loci (Manis et al., 2004; Ward et al., 2004; Reina-San-Martin et al., 2007). In addition, loss of 53BP1 leads to impaired distal V-DJ joining (Difilippantonio et al., 2008). Furthermore, chromosome fusions of Trf2-uncapped telomeres by classical nonhomologous end-joining (NHEJ) require 53BP1 (Rai et al., 2010). Additionally, defects in distal joining of dysfunctional telomeres via NHEJ are seen in the absence of 53BP1 (Dimitrova et al., 2008). Notably, recent work has shown that 53BP1 deficiency rescues phenotypes associated with BRCA1 dysfunction. Thus, depletion of 53BP1 rescues the proliferation defect observed in *Brcal*-null cells and the hypersensitivity of *Brcal*-null cells to cisplatin and mitomycin C (Bouwman et al., 2010). Loss of 53BP1 also alleviates the hypersensitivity of *Brcal* mutant cells to PARP inhibition and allows for processing of DNA ends to promote homologous recombination (Bunting et al., 2010).

Here, we investigate the accumulation of 53BP1 in large nuclear bodies within a subset of asynchronously growing mammalian cells. Specifically, we reveal that these bodies represent previously characterized OPT (Oct-1, PTF, transcription) domains (Pombo et al., 1998), as 53BP1 colocalizes in these structures together with Oct-1 and PTF in G1 cells. In addition to showing that 53BP1-OPT domains represent sites of low transcriptional activity, we establish that their integrity depends on H2AX and the protein kinase activity of ataxia telangiectasia mutated (ATM). Consistent with these data, we demonstrate that 53BP1-OPT domains also contain phosphorylated H2AX (γ H2AX) and mediator of DNA damage checkpoint 1 (MDC1), which strongly suggests that these domains represent sites of DNA damage. Finally, we establish that although 53BP1-OPT domains are restricted to G1 cells, their formation is enhanced by exposure of cells to APH. We discuss these findings in relation to the molecular events leading to OPT domain formation and disassembly, as well as their potential functions in maintaining genome integrity.

Results

53BP1 accumulates in nuclear bodies in G1 cells

Although it is well established that 53BP1 localizes to sites of DNA DSBs generated when cells are treated with DNA damaging agents, we and others have known for several years (Morales et al., 2003; Doil et al., 2009) that 53BP1 localizes to a small number of large (2–3 μ m) discrete bodies/foci in the nuclei of tissue culture cells grown under normal conditions (Fig. 1 A). Because these bodies occur in only a subset of cells within an asynchronously growing population, we explored whether 53BP1 body formation was cell cycle dependent. Thus, we performed immunofluorescence studies in several human and murine cell lines with an antibody against Cyclin A (Cyc A) as a marker of S/G2 phases. Strikingly, the large majority of cells containing large 53BP1 nuclear bodies were Cyc A negative (Fig. 1 A and not depicted). Furthermore, quantification of Cyc A-negative cells with large 53BP1 bodies in telomerized (human telomerase reverse transcriptase [hTERT]) human BJ fibroblasts revealed that 16% of total cells and 21% of

Cyc A-negative cells contained such bodies (Fig. 1 B). Of the Cyc A-negative cells containing 53BP1 bodies, 87% contained one body, whereas 11% and 2% contained two and more than two bodies, respectively (Fig. 1 B). In parallel studies, we found that 53BP1 nuclear bodies also existed in a subset of quiescent primary human fibroblasts (unpublished data). Collectively, these data revealed that large 53BP1 nuclear bodies occur preferentially in G0 and G1 cells.

To further characterize the formation of 53BP1 nuclear bodies in G1, we used human U2OS cells stably expressing 53BP1 fused to EGFP. Live cell imaging revealed that when 53BP1 bodies arose, they did so almost immediately after a mitotic cell entered G1 phase, and that in most cases (>90%), the bodies arose in parallel within both daughter cells (Fig. 1 C). Furthermore, when we pulsed cells with 5-ethynyl-2'-deoxyuridine (EdU) to mark sites of DNA replication, we observed that 53BP1 bodies were invariably EdU negative (Fig. 1 D). In accordance with our other data, this analysis revealed that although no large 53BP1 bodies were present in S phase cells, smaller 53BP1 nuclear foci existed in a fraction of early S phase cells (14%) and mid S phase cells (3%) but were absent in late S phase cells (Fig. 1 D). Collectively, these findings suggested that 53BP1 nuclear bodies are either removed, or do not form effectively, in mid or late S phase cells. This conclusion was supported by live imaging studies of U2OS cells stably expressing EGFP-53BP1 and mRuby-PCNA, where we observed that large nuclear 53BP1 bodies present in G1 cells gradually disappeared as S phase progression ensued (Fig. 1 E).

53BP1 is a component of OPT domains

To determine whether 53BP1 nuclear bodies are related to one of the various subnuclear bodies/domains that have been previously documented (Spector, 2006), we used antibodies specific for such domains to see whether they colocalized with 53BP1. Thus, by staining with an antibody against fibrillarin, we found that 53BP1 nuclear bodies did not reside in the nucleolus and that, in fact, 53BP1 nuclear staining was consistently excluded from the nucleolus (Fig. S1). In addition, we found that 53BP1 bodies did not colocalize with Cajal bodies as detected by coilin staining. Furthermore, 53BP1 nuclear bodies were not components of splicing speckles containing the SC-35 protein, although we did note that 53BP1 bodies frequently had SC-35 staining adjacent to them (Fig. S1).

As 53BP1 nuclear bodies are quite large in size (2–3 μ m) and are cell cycle regulated, we explored whether they might correspond to OPT domains that share similar size and cell cycle characteristics, and which contain the transcription factors Oct-1 and PTF (Pombo et al., 1998). Strikingly, we observed that 53BP1 nuclear bodies colocalized with staining produced by antibodies against Oct-1 and two different subunits of PTF (PTF δ and PTF γ) in BJ fibroblasts (Fig. 2 A). Consistent with earlier work (Pombo et al., 1998), we also found that a PML body often resided at the periphery of, or was contained within, 53BP1 nuclear bodies (Fig. 2 A). In addition, similar colocalizations between 53BP1 and Oct-1, PTF δ , or PML were observed in U2OS cells (Fig. 2 B). Collectively, these results established that 53BP1 is a component of the previously described

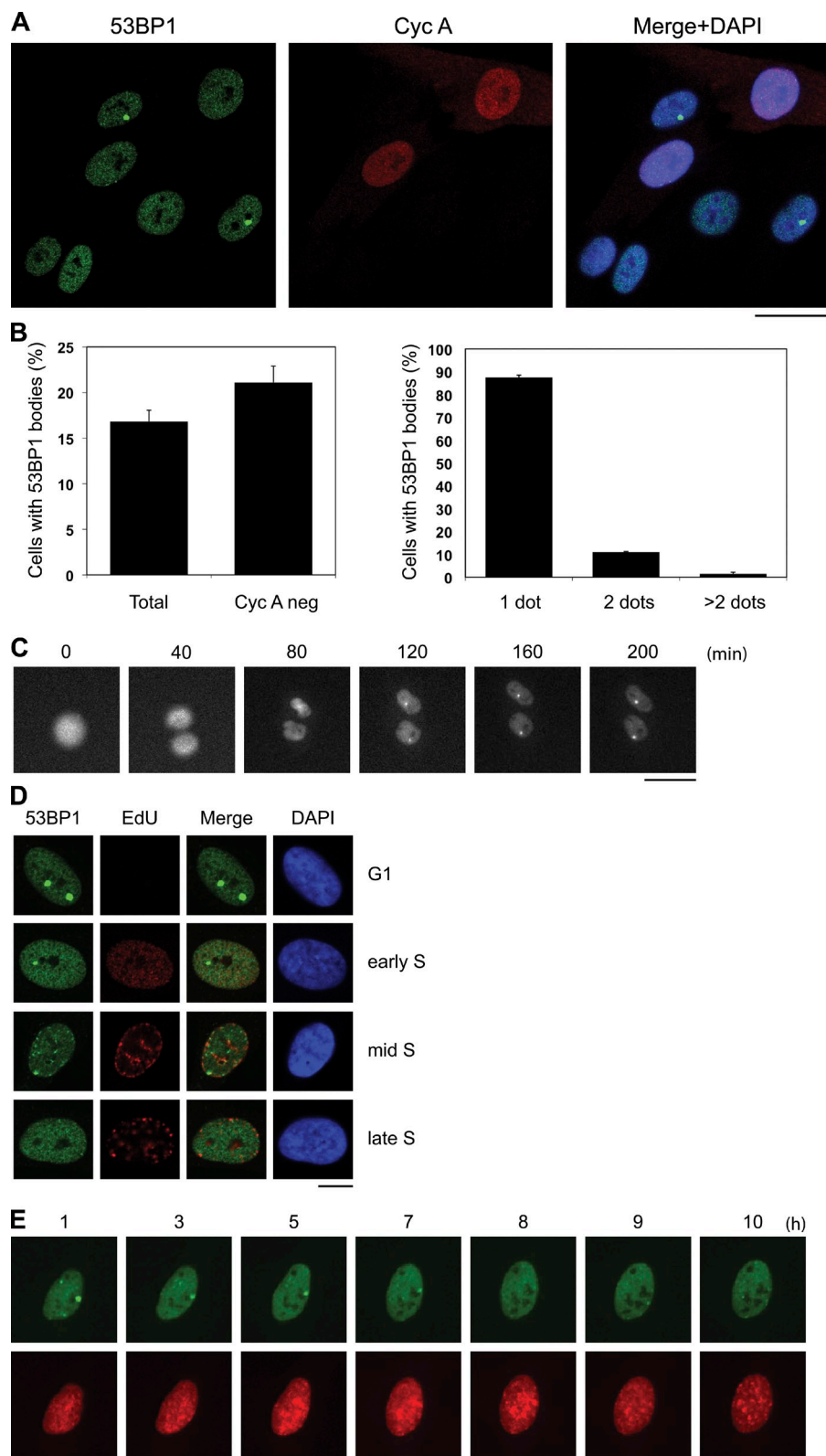


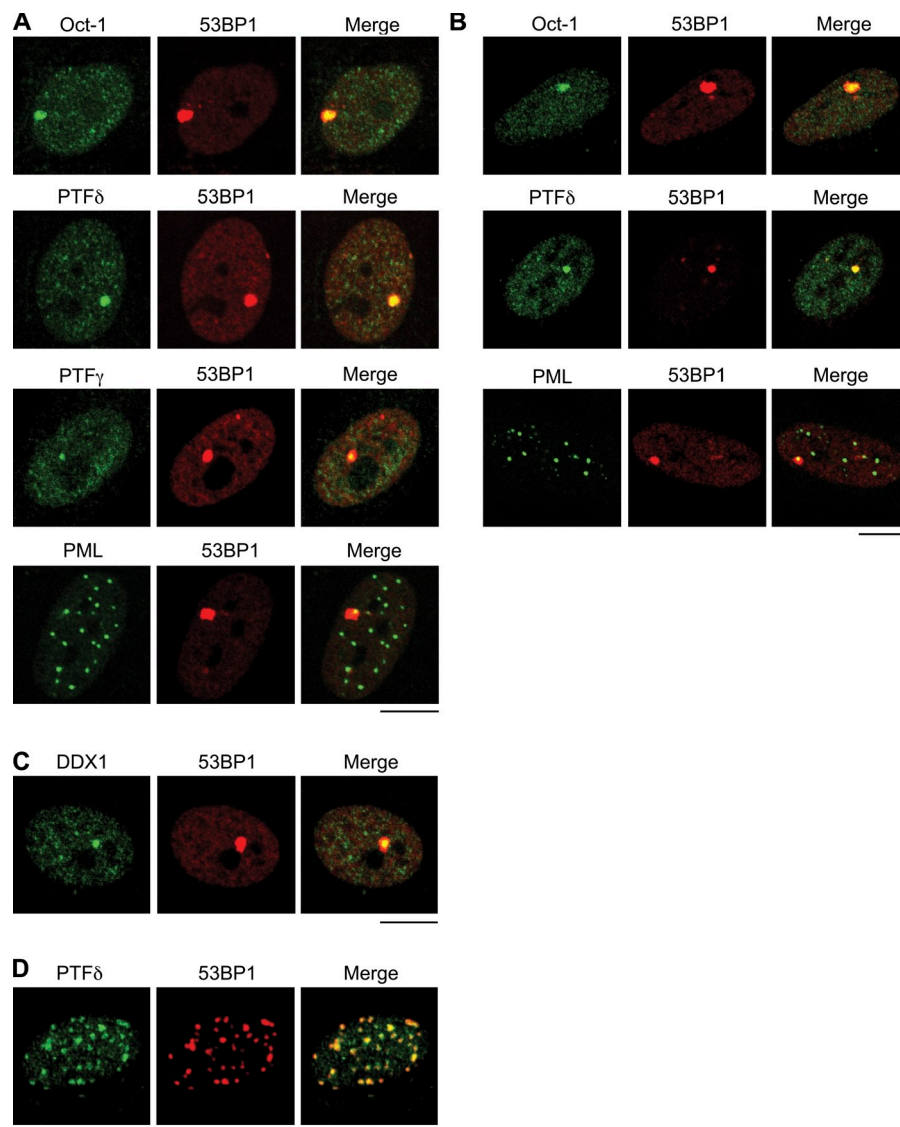
Figure 1. 53BP1 accumulates in nuclear bodies in a subset of G1 cells. (A) Asynchronously growing BJ hTERT cells were fixed, and immunofluorescence was performed with mouse anti-53BP1 and rabbit anti-Cyc A antibodies. (B, left) Quantitation of total or Cyc A-negative cells from A that contained 53BP1 nuclear bodies. Results represent the mean \pm SD from three experiments (total, $n = 4,944$; Cyc A negative, $n = 3,956$). (B, right) Quantitation of Cyc A-negative cells from A that contained 53BP1 bodies. Results represent the mean \pm SD from three experiments ($n = 829$). We note that 53BP1 foci were also observed in 10.8% ($\pm 2.8\%$) of Cyc A-positive cells (not depicted), which likely represent early-to-mid S phase cells (see D). (C) Live cell imaging of U2OS cells stably expressing EGFP-53BP1 from mitosis into G1. (D) BJ hTERT cells were pulsed with EdU for 10 min, fixed, and stained with rabbit anti-53BP1 antibodies. EdU was visualized using click chemistry. (E) Live cell imaging of U2OS cells stably expressing EGFP-53BP1 and mRuby-PCNA from G1 into S phase. Bars: (A and C) 30 μ m; (D and E) 10 μ m.

OPT domain. While surveying for additional colocalizing factors, we found that the DEAD box RNA/RNA and RNA/DNA helicase DDX1 also localized with 53BP1 nuclear bodies (Fig. 2 C), showing that previously characterized DDX1 bodies (Li et al., 2006) in G1 cells are also components of 53BP1-OPT domains.

53BP1-OPT domains require DNA damage signaling and exhibit low transcription levels

Previous work has established that DNA DSBs trigger activation of the phosphoinositide 3-kinase-related protein kinases (PIKKs) ATM, ATR, and DNA-PK (Lempiäinen and

Figure 2. 53BP1 colocalizes with components of OPT domains. (A) Immunofluorescence was performed in BJ primary or BJ hTERT (PTF γ) fibroblasts with mouse anti-53BP1 and rabbit anti-Oct-1, anti-PTF δ , or anti-PTF γ , and rabbit anti-53BP1 and mouse anti-PML antibodies as indicated. Analysis of >100 cells revealed that 88% of 53BP1 nuclear bodies contained at least one PML body. (B) Experiments were performed as in A with U2OS cells and the indicated antibodies. (C) Immunofluorescence was performed in BJ primary fibroblasts with mouse anti-53BP1 and rabbit anti-DDX1 antibodies. (D) BJ hTERT fibroblasts were exposed to 1.5 Gy of ionizing radiation and fixed 1 h later. Immunofluorescence was performed with rabbit anti-PTF δ and mouse anti-53BP1 antibodies. Bars, 10 μ m.



Halazonetis, 2009; Lovejoy and Cortez, 2009), which then phosphorylate various proteins, including the histone variant H2AX. γ H2AX then recruits MDC1, which is required for the effective accumulation and retention of 53BP1 at DSB sites (Celeste et al., 2003; Stucki and Jackson, 2006). Notably, we found that 53BP1-OPT domains colocalized with both γ H2AX and MDC1 (Fig. 3 A), which strongly suggests that they correspond to sites of DNA damage. In accord with this, the proportion of cells with 53BP1 nuclear bodies in Cyc A–negative cells was substantially lower in H2AX^{−/−} mouse embryonic fibroblasts (MEFs) than in wild-type controls (Fig. 3 B). In addition, we found that 53BP1 nuclear bodies, as detected by 53BP1 staining (Fig. 3 C) or staining with other OPT domain components (PTF δ and PML; Fig. 3 D), were largely abrogated when asynchronously growing BJ cell populations were incubated with the ATM inhibitor KU-55933 (Hickson et al., 2004). In contrast, we found that 53BP1 formed large nuclear bodies that colocalized with PTF δ and PML within Cyc A–negative ATR-deficient Seckel cells (Fig. S2). However, we note that immunofluorescence studies revealed the presence of OPT

domains, albeit smaller in size, in both ATM-deficient AT cells and ATM^{−/−} MEFs (unpublished data), which suggests that, although OPT domain formation is largely ATM dependent, other PIKKs such as DNA-PK and/or ATR are also likely to contribute, particularly when ATM is absent. Collectively, these data strongly suggested that 53BP1-OPT domains represent sites of endogenously arising DNA damage in G1 cells. In line with this idea, we found that Oct-1, PTF δ , and PTF γ were recruited to tracts of DNA damage produced by laser micro-irradiation (Fig. S3 A). PTF δ also formed foci that colocalized with 53BP1 in cells treated with ionizing radiation (Fig. 2 D), whereas PML did not (Fig. S3 B). These results thus provided additional support for OPT domains being sites of DNA damage and suggested roles for various OPT domain components in the DDR.

Recent work has shown that transcription is inhibited at DNA DSB sites by mechanisms requiring ATM kinase activity (Shanbhag et al., 2010). Consistent with 53BP1-OPT domains in G1 cells corresponding to DNA damage sites, they did not colocalize with initiating or elongating forms of RNA polymerase II (Pol II), as detected by antibodies recognizing phosphorylated

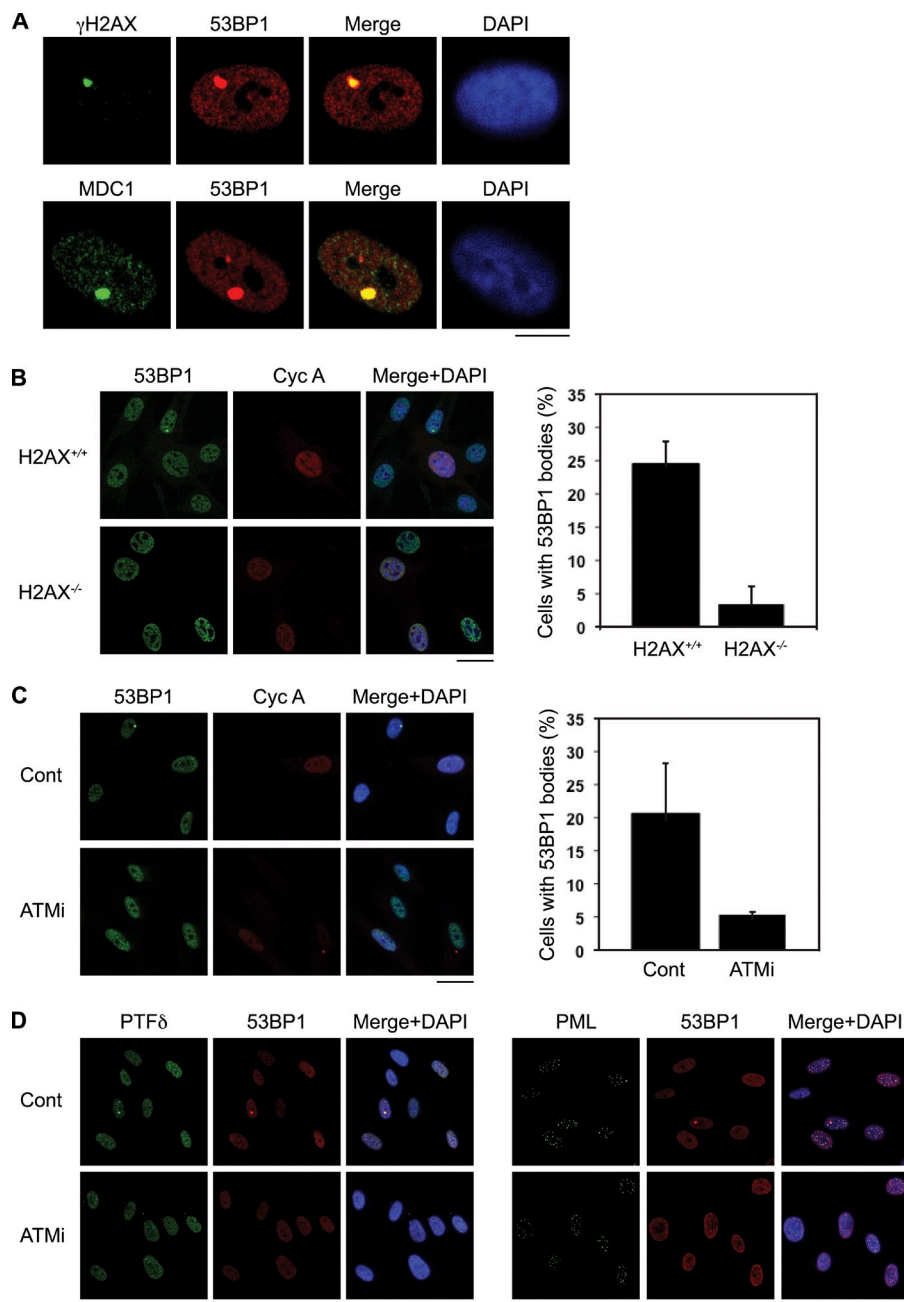


Figure 3. 53BP1-OPT domains represent sites of DNA damage. (A) Immunofluorescence was performed in BJ hTERT fibroblasts with rabbit anti-53BP1 and mouse anti- γ H2AX (top) or mouse anti-53BP1 and rabbit anti-MDC1 pSDTD (bottom) antibodies. (B, left) Immunofluorescence was performed in H2AX^{+/+} or H2AX^{-/-} MEFs with rabbit anti-53BP1 or mouse anti-Cyc A antibodies. (B, right) Quantitation of Cyc A-negative cells that contained 53BP1 nuclear bodies. Results represent the mean \pm SD from three experiments (H2AX^{+/+}, $n = 636$; H2AX^{-/-}, $n = 384$). (C, left) BJ hTERT fibroblasts were incubated in the absence (Cont) or presence of ATM inhibitor KU55933 (ATMi; 20 μ M) for 3 h. Immunofluorescence was performed with mouse anti-53BP1 and rabbit anti-Cyc A antibodies. (C, right) Quantitation of Cyc A-negative cells that contained 53BP1 nuclear bodies. Results represent the mean \pm SD from three experiments (Cont, $n = 522$; ATMi, $n = 491$). (D) Experiments were performed as in C and immunofluorescence was performed with rabbit anti-PTF δ and mouse anti-53BP1 antibodies (left) or mouse anti-PML and rabbit anti-53BP1 antibodies (right). Bars: (A) 10 μ m; (B–D) 30 μ m.

Ser-5 (pS5) and Ser-2 (pS2) within the C-terminal domain of the Pol II large subunit (Fig. 4 A). Moreover, when we used incorporation of 5-fluorouridine (FIU) to detect sites of active transcription, this revealed that 53BP1-OPT domains were largely devoid of FIU staining (Fig. 4 B). In addition, we observed that 53BP1 nuclear bodies were lost when cells were treated with DNase I but not RNase A before immunofluorescence staining (Fig. 4 C and not depicted). Collectively, these results demonstrated that 53BP1-OPT domains associate with DNA but do not correspond to sites of detectable transcription.

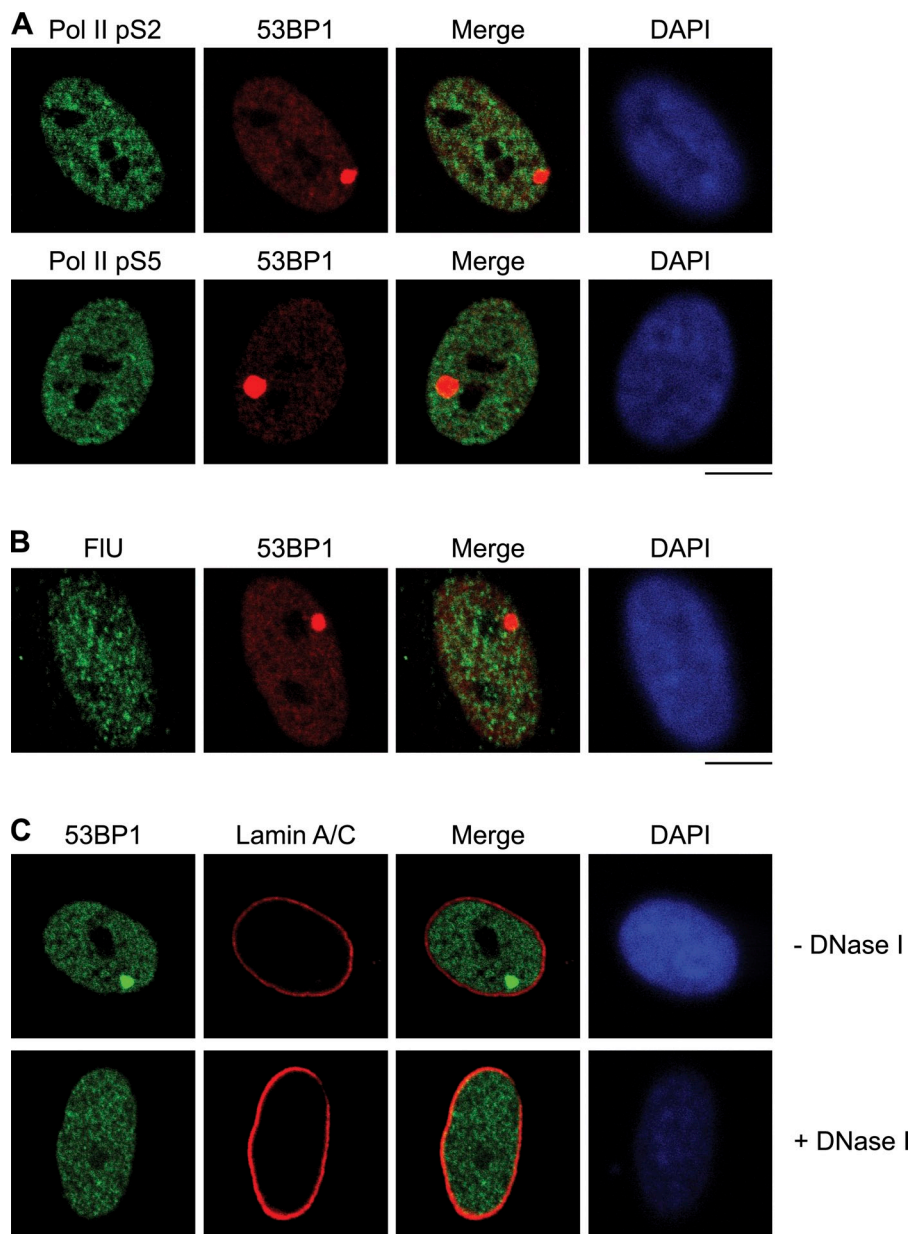
Links between 53BP1-OPT domains and chromosomal fragile sites

To determine whether OPT domains containing 53BP1 are preferentially associated with particular chromosomal regions,

we performed DNA immuno-FISH experiments. By using whole chromosome paints specific for seven different chromosomes, we found that 53BP1-OPT domains colocalized with chromosome 2 in \sim 45% of cells with these domains (Fig. 5 A and Table I). These data were therefore consistent with a previous study by Pombo et al., (1998), which showed that PTF domains displayed the highest level of colocalization with chromosome 2. Furthermore, our analyses revealed that $>$ 30% of cells containing 53BP1-OPT domains colocalized with chromosomes 3, 6, or 7 (Fig. 5 A and Table I).

To more precisely map the genomic regions containing OPT domains, we performed chromatin immunoprecipitation experiments followed by massively parallel sequencing (ChIP-seq; Robertson et al., 2007). Because we have observed that the majority of 53BP1 is chromatin bound (resistant to extraction

Figure 4. 53BP1-OPT domains do not associate with regions of active transcription and are dependent on DNA. (A) Immunofluorescence was performed in BJ primary fibroblasts with mouse anti-53BP1 and rabbit anti-Pol II pS2 (top) or rabbit anti-53BP1 and mouse anti-Pol II pS5 (bottom) antibodies. (B) BJ primary fibroblasts were incubated for 60 min with FIU and immunofluorescence was performed with rabbit anti-53BP1 and mouse anti-BrdU antibodies. (C) BJ primary fibroblasts were incubated in the absence or presence of DNase I as indicated for 10 min. Immunofluorescence was performed with rabbit anti-53BP1 or mouse anti-Lamin A/C antibodies. DAPI and Lamin A/C were positive and negative controls, respectively. Bars, 10 μ m.



with 400 mM salt) even when cells are grown in the absence of DNA damaging agents (unpublished data) and because cells containing OPT domains only represent a minority (\sim 16%) of the total cell population, we reasoned that ChIP-seq analysis of 53BP1 itself would not be OPT domain specific. Therefore, we performed experiments on serum-starved BJ hTERT fibroblasts with antibodies against γ H2AX, as this phospho-epitope is highly specific to OPT domains in G0 cells that have not been treated with a DNA damaging agent. By comparing data sets derived from immunoprecipitated γ H2AX samples with those from control immunoglobulin immunoprecipitations, we found that γ H2AX was specifically associated with various specific regions of the genome in G0 arrested cells (Fig. 5 and Table II). The genomic locations of the top eight γ H2AX-association peaks (as determined by fold enrichment) were located on chromosomes 1 (1q23.2), 2 (2p24.2), 7 (7p13, 7q22.3), 9 (9q33.3), 19 (19p13.3), 20 (20q13.33), and 21 (21q22.3), with four of

these peaks corresponding to known common fragile sites (FRA2C, FRA7D, FRA7F, and FRA19B; Schwartz et al., 2006; Durkin and Glover, 2007). Collectively, the DNA immunofluorescence and ChIP-seq results therefore indicated enhanced associations of OPT domains with chromosomes 2 and 7 in human fibroblasts and, moreover, suggested that these domains preferentially localize to chromosomal fragile sites.

Chromosomal fragile sites are induced by treating cells with low doses of APH, whereas other replication-inhibiting drugs such as hydroxyurea (HU) are less specific at inducing common fragile site lesions (Durkin and Glover, 2007). Thus, we hypothesized that DNA damage arising from unreplicated or partially replicated genomic regions might be responsible for the formation of 53BP1-OPT domains in G1 cells. Consistent with this, incubation of cells for 24 h with a low concentration of APH (0.4 μ M) produced a marked increase in both the proportion of Cdc 2–negative cells containing 53BP1 nuclear bodies

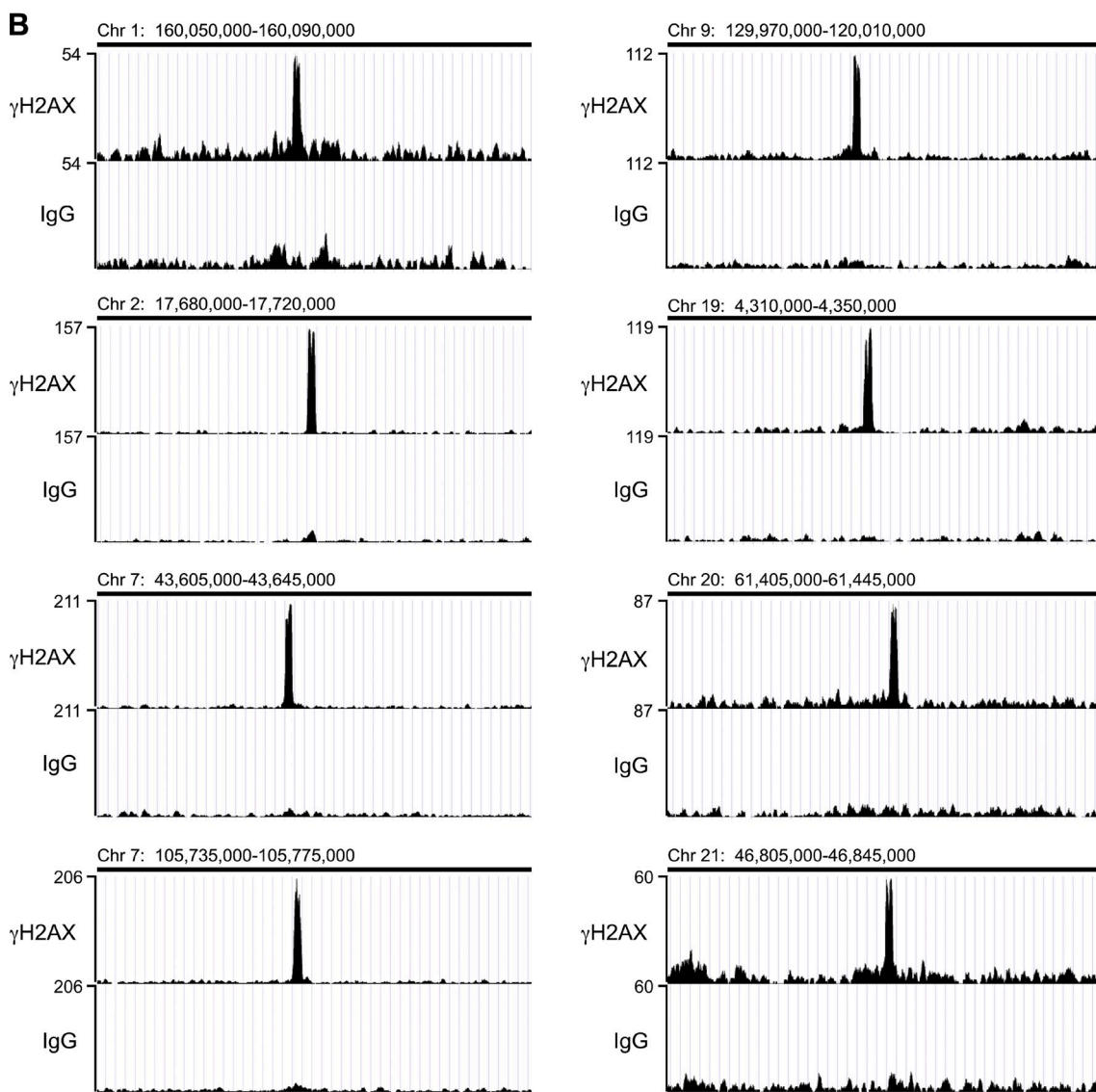
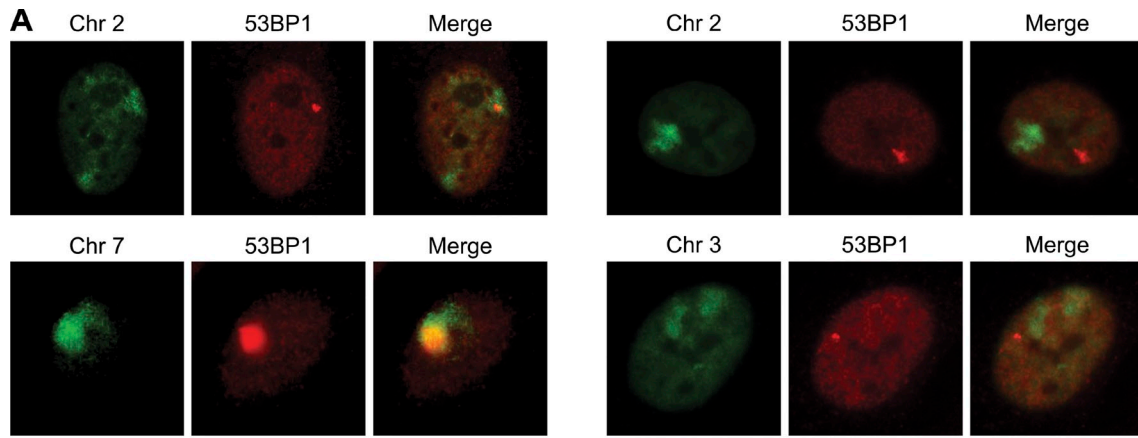


Figure 5. γ H2AX accumulates at discrete regions of the genome in untreated cells. (A) DNA Immuno-FISH was performed in BJ hTERT fibroblasts with anti-53BP1 antibodies and whole chromosome paints. (A, left) Colocalization between 53BP1 nuclear bodies and chromosome regions. (A, right) No colocalization between 53BP1 nuclear bodies and chromosome regions. Bar, 10 μ m. (B) ChIP-seq experiments were performed with serum-starved (G0) BJ hTERT fibroblasts and γ H2AX antibodies. The eight highest peaks for γ H2AX enrichment are displayed along with the negative control (IgG). Data are shown as custom tracks (bin 20) on the UCSC genome browser (data correspond to the Feb. 2009 GRCh37/hg19 genome assembly). The axis scales are presented on the left and chromosome position at the top.

Table I. Frequency of association between chromosomes and 53BP1-OPT domains

Chromosome number	Chromosome size	Colocalization with 53BP1-OPT domains		No colocalization with 53BP1-OPT domains	
	<i>Mb</i>	%		%	
2	243	45 (<i>n</i> = 168)		55 (<i>n</i> = 203)	
3	198	41 (<i>n</i> = 129)		59 (<i>n</i> = 188)	
6	171	32 (<i>n</i> = 113)		68 (<i>n</i> = 241)	
7	159	36 (<i>n</i> = 105)		64 (<i>n</i> = 194)	
14	107	26 (<i>n</i> = 79)		74 (<i>n</i> = 235)	
16	90	27 (<i>n</i> = 99)		73 (<i>n</i> = 261)	
17	81	24 (<i>n</i> = 81)		76 (<i>n</i> = 254)	

Results represent the average of two independent experiments. *n* = number of cells analyzed.

and the number of these bodies per cell (Fig. 6, A and B). We note that under these conditions, ~8% of Cyc A-positive cells also contained 53BP1 foci. Low APH doses also increased the number of PTFδ domains, which colocalized with 53BP1, as well as an increased association of 53BP1 with PML bodies (Fig. S4). Treatment of cells with a higher dose of APH (4 μM) produced similar results (unpublished data), although the ensuing numbers of 53BP1 nuclear bodies per cell were even higher.

In contrast to our observations after APH treatment, incubation with HU did not significantly affect the incidence of

53BP1-OPT domains as a percentage of total cells, or the number of these domains per cell. However, a slightly increased proportion of Cyc A-negative cells displaying 53BP1-OPT domains was observed after HU treatment (Fig. 6 C). Importantly, the differences observed between APH and HU did not reflect differences in the extent of S phase perturbation, as both agents caused a similar accumulation of cells in S/G2 phase (from 27% in control cells to 46% and 52% in APH- and HU-treated cells, respectively), as determined by flow cytometry (Fig. 6 D). Furthermore, as shown in Fig. 6 E, incubation with either agent resulted

Table II. CHIP-seq peaks for γH2AX

Chromosome number	Start position	End position	Chromosome position	Fragile site
1	79171862	79172697	1p31.1	
1	160068001	160069262	1q23.2	
1	180991672	180992627	1q25.3	FRA1G
2	17699186	17700299	2p24.2	FRA2C
2	196527371	196527999	2q32.3	
2	242823452	242824274	2q37.3	FRA2J
4	155337857	155338768	4q31.3	
5	54095885	54096590	5q11.2	
5	148822299	148823429	5q32	
6	37137202	37138474	6p21.2	
7	6542950	6544002	7p22.1	FRA7B
7	43622016	43623713	7p13	FRA7D
7	105751952	105753887	7q22.3	FRA7F
8	143858334	143859358	8q24.3	FRA8D
9	129986095	129988041	9q33.3	
10	99599623	99600560	10q24.2	
11	133906686	133907757	11q25	
12	117565420	117567081	12q24.22	
16	2954968	2956441	16p13.3	
16	22201426	22202642	16p12.2	
17	15163610	15165033	17p12	FRA17A
17	17109369	17110420	17p11.2	
17	70404690	70406426	17q24.3	
17	73829429	73831182	17q25.1	
17	75276722	75278117	17q25.2	
19	1122785	1123630	19p13.3	FRA19B
19	4327867	4329218	19p13.3	FRA19B
19	53030425	53031358	19q13.4	
20	61424927	61426403	20q13.33	
20	62272821	62273976	20q13.33	
21	46824896	46826026	21q22.3	
22	45636492	45637492	22q13.31	FRA22A

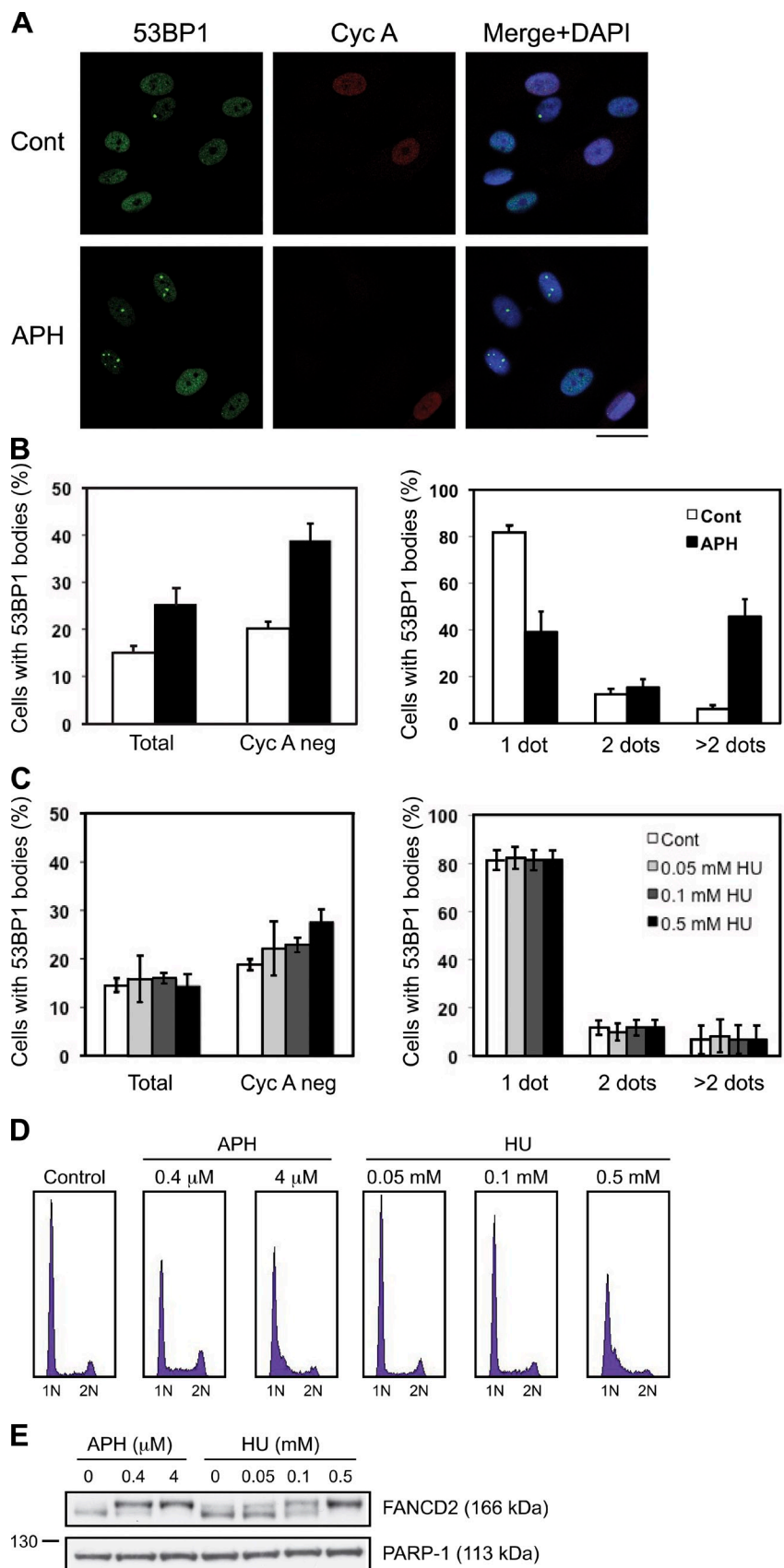


Figure 6. Replication perturbation by APH promotes formation of 53BP1-OPT domains. (A) BJ hTERT fibroblasts were incubated in the absence (Cont) or presence of APH (0.4 μM, 24 h) as indicated. Immunofluorescence was performed using mouse anti-53BP1 and rabbit anti-Cyc A antibodies. Bar, 30 μm. (B, left) Quantitation of total or Cyc A-negative cells from A that contained 53BP1 nuclear bodies. Results represent the mean ± SD from three experiments (total: Cont, *n* = 1,329; APH, *n* = 1,291; Cyc A negative: Cont, *n* = 987; APH, *n* = 843). (B, right) Quantitation of Cyc A-negative cells from A that contained 53BP1 nuclear bodies. Results represent the mean ± SD from three experiments (Cont, *n* = 199; APH, *n* = 328). (C) BJ hTERT fibroblasts were incubated in the absence (Cont) or presence of HU for 24 h as indicated. Immunofluorescence was performed as described in A and quantified as in B. Results represent the mean ± SD from three experiments. (D) FACS analysis of cells incubated in the absence or presence of APH or HU as indicated. (E) Cellular lysates from cells treated with APH or HU as in A and C were separated by SDS-PAGE, and Western blotting was performed with antibodies against FANCD2 and PARP-1 (loading control).

in a marked increase in the mono-ubiquitylation of FANCD2, a well-characterized marker of replication stress (Howlett et al., 2005). Thus, although exposure to both APH and HU partially inhibited DNA synthesis, only APH treatment increased the number of 53BP1-OPT domains in G1 cells. Collectively, our findings thereby indicated that 53BP1-OPT domains represent genomic loci that exhibit intrinsic replication difficulties, such as common fragile sites.

Discussion

We have established that 53BP1 is a new component of previously characterized OPT domains (Pombo et al., 1998), as it colocalizes with Oct-1 and PTF in large nuclear bodies of G1 cells. Consistent with what has been reported for OPT domains (Pombo et al., 1998), we found that 53BP1 nuclear bodies form early in G1 and then dissociate as cells enter and progress through S phase. Moreover, we show that localization of 53BP1 to OPT domains depends on H2AX and is largely abrogated by ATM inhibition, which, together with the colocalization of 53BP1-OPT domains with γ H2AX and MDC1, strongly suggests that these domains arise at sites of DNA damage. Although the presence of transcription factors Oct-1 and PTF in OPT domains has been taken as evidence that these represent sites of active transcription (Pombo et al., 1998), we find that 53BP1-OPT domains are largely devoid of the phosphorylated, elongating forms of Pol II, and lack detectable transcription as assessed by FIU labeling. These data are therefore in line with recent studies showing that DNA damage causes localized inhibition of transcription (Iacovoni et al., 2010; Shanbhag et al., 2010). In this regard, it is noteworthy that we have found that the RNA helicase DDX1 resides in 53BP1-OPT domains, and that this factor localizes to sites of DNA damage that do not contain newly synthesized RNA (Li et al., 2008). Collectively, our results therefore demonstrate that OPT domains contain DNA damage signaling proteins and therefore likely mark sites of DNA damage.

In light of our data indicating that 53BP1-OPT domains are induced by APH and enriched at certain chromosomal fragile sites, we suggest that 53BP1-OPT domains assemble on, and arise as a consequence of, sites of impaired replication from the previous S phase. Such incompletely replicated regions could arise through the actions of drugs such as APH, endogenously arising DNA damaging agents, or because of intrinsic replication difficulties at particular genomic loci. In this regard, it is noteworthy that recent work from Chan et al. (2009) has shown that APH treatment induces FANCD2 sister foci in metaphase chromosomes that colocalize with fragile site loci. Furthermore, \sim 10% of the FANCD2 sister foci observed in metaphase cells associate with Bloom syndrome helicase (BLM)-coated ultrafine bridges during anaphase (Chan et al., 2009). Collectively with these findings, our data suggest a model whereby certain regions of the genome, particularly those associated with chromosomal fragile sites, may remain unreplicated during S phase. Such regions would then be bound by the Fanconi anemia proteins FANCD2 and FANCI during G2 phase and upon entry into mitosis. During anaphase, BLM, together with topoisomerase III α and hRMI1, would then resolve the partially replicated, hemicatenated DNA (Chan et al., 2007), and upon entry into G1,

the unreplicated DNA intermediate would be recognized as DNA damage, resulting in the establishment of 53BP1-OPT domains.

Although the above model suggests that the OPT domains would contain large stretches of single-stranded DNA (ssDNA), we note that we have not been able to detect the presence of ssDNA in 53BP1-OPT domains by immunofluorescence staining for RPA or for BrdU incorporation under nondenaturing conditions (Sartori et al., 2007; unpublished data). Thus, if ssDNA does exist in 53BP1-OPT domains, it must either be bound by proteins that we have not yet examined and/or must adopt secondary structures that preclude ssDNA detection. In this regard, we note that the ssDNA overhang of telomeres is bound by protein components of the Shelterin complex and is sequestered by the formation of a T-loop (Palm and de Lange, 2008). We therefore speculate that the sequestration of ssDNA regions within 53BP1-OPT domains may provide a mechanism to prevent their repair by relatively error-prone gap-filling polymerases in G1 and allow progression into S phase, where such stretches of ssDNA could then be faithfully filled in by replicative polymerases. Nevertheless, we are unable to exclude the possibility that, during the segregation of chromosomes during mitosis, unreplicated regions that are not resolved instead result in DNA DSBs. If this is the case, the persistence of OPT domains throughout G1 would imply that such DSBs are not repaired in G1, possibly because they require processing by factors that are not present in G1 or require modification by cyclin-dependent kinases as cells progress from G1 into S phase. Whatever the case, our data yield a model in which impaired DNA synthesis during S phase leads to activation of a DDR and the formation of 53BP1-OPT domains in the subsequent G1 in order to maintain genome integrity.

Materials and methods

Cell culture and treatments

Human BJ primary fibroblasts, BJ hTERT immortalized fibroblasts, and Seckel cells were cultured in DME (Invitrogen) supplemented with 15% FBS, penicillin, streptomycin, glutamine, and fungazone (PSQF). Human U2OS osteosarcoma cells and H2AX^{-/-} and H2AX^{+/+} MEFs (provided by A. Nussenzweig, National Cancer Institute, National Institutes of Health, Bethesda, MD) were maintained in DME plus 10% FBS and PSQF. U2OS cells stably expressing pEGFP-53BP1 (Galanty et al., 2009) were grown in DME plus 10% FBS, PSQF, and G418 (500 μ g/ml). U2OS cells stably expressing EGFP-53BP1 and mRuby-PCNA (provided by P. Marco-Casanova, The Gurdon Institute, University of Cambridge, Cambridge, England, UK) were grown in DME plus 10% FBS, PSQF, G418 (500 μ g/ml), and 0.25 μ g/ml puromycin.

Cells were incubated with APH (Sigma-Aldrich) or HU (Sigma-Aldrich) for 24 h as indicated. For inhibition of ATM, cells were incubated with the specific ATM inhibitor KU55933 (Hickson et al., 2004) at 20 μ M for 3 h before fixation. To identify transcriptionally active regions, cells were incubated with 5 mM FIU (Sigma-Aldrich) for 60 min before fixation. Cells were irradiated using a Faxitron x-ray cabinet at 3.15 Gy/min.

Immunofluorescence microscopy

Cells were grown on glass coverslips and fixed with one of the following methods: ice-cold MeOH/acetone for 10 min at RT, 2% paraformaldehyde (PFA) for 15 min at RT followed by incubation with 0.5% Triton X-100 in PBS for 10 min at RT, 4% formaldehyde (FA; Sigma-Aldrich) in PBS for 15 min at RT followed by incubation with 0.5% Triton X-100 in PBS for 10 min at RT, or pre-extraction buffer (25 mM HEPES, pH 7.4, 50 mM NaCl, 1 mM EDTA, 3 mM MgCl₂, 300 mM sucrose, and 0.5% Triton X-100) for 5 min at RT followed by fixation with 2% PFA for 15 min at RT. After fixation, cells were washed with PBS and blocked with either 5% FBS in PBS or 5% BSA in PBS. Cells were incubated with primary antibodies (1 h at RT or overnight at 4°C)

in blocking buffer, washed with PBS, and then incubated with Alexa Fluor 488 goat anti-mouse/rabbit and Alexa Fluor 594 goat anti-mouse/rabbit (Invitrogen) for 1 h at RT in blocking buffer. DNA was counterstained with DAPI in Vectashield mounting agent (Vector Laboratories). Images were acquired using a laser scanning system (Radiance 2100; Bio-Rad Laboratories) on a microscope (Eclipse E800 upright; Nikon) using a 40 \times objective lens and Lasersharp 2000 software (Carl Zeiss, Inc.).

For DNase treatments, cells grown on coverslips were washed with CSK buffer (10 mM Pipes, pH 7, 100 mM NaCl, 300 mM sucrose, and 3 mM MgCl₂) and incubated with CSK buffer plus 0.5% Triton X-100 in the absence or presence of DNase I (Roche; 200 U/ml in 10 mM Hepes, pH 7.4, 50 mM KCl, 10% glycerol, and 1.5 mM MgCl₂) for 10 min at RT. Coverslips were subsequently washed and fixed with 4% FA in PBS for 15 min at RT, and immunostained as described above.

To detect S phase cells by EdU labeling, BJ hTERT cells were grown on glass coverslips and pulse-labeled for 10 min by supplementing the cell culture medium with 50 μ M EdU (Invitrogen). The cells were fixed for 10 min with 4% FA in PBS and permeabilized with 0.5% Triton X-100/PBS for 10 min at RT. EdU was stained with Alexa Fluor 594 azide (Invitrogen) via click chemistry reaction (Salic and Mitchison, 2008) broadly following the manufacturer's recommendations as described previously (Dimitrova, 2009).

Laser micro-irradiation was used to generate localized damage in cellular DNA by exposure to a UVA laser beam as described previously (Ahel et al., 2009). In brief, cells were plated on glass-bottomed dishes (WillCo) and sensitized with 10 μ M BrdU (Sigma-Aldrich) in phenol red-free medium (Invitrogen) for 24 h at 37°C. Laser micro-irradiation was performed on a confocal microscope (FluoView 1000; Olympus) equipped with a 37°C heating stage (Ibidi) and a 405-nm laser diode (6 mW, SIM scanner) focused through a 60 \times UPlan-SApochromat/1.35 NA oil objective lens to yield a spot size of 0.5–1 μ m. After 1 h, cells were fixed and immunostained as indicated.

Antibodies used for immunofluorescence were: 53BP1 (mouse; a gift from T. Halazonetis, University of Geneva, Geneva, Switzerland), 53BP1 (mouse; a gift from J. Chen, University of Texas MD Anderson Cancer Center, Houston, TX), 53BP1 (rabbit, NB100-304; Novus Biologicals), Cyc A (rabbit, H432; Santa Cruz Biotechnology, Inc.), Cyc A (mouse; CRUK), Oct-1 (Zwilling et al., 1994), PTF δ (Pombo et al., 1998), PML (mouse, PG-M3; Santa Cruz Biotechnology, Inc.), PTF γ (rabbit, CS48; a gift from N. Hernandez, University of Lausanne, Lausanne, Switzerland), DDX1 (Li et al., 2008), γ H2AX (mouse, 05-636; Millipore), MCD1 pSDTD (Chapman and Jackson, 2008), fibrillarin (mouse; Millipore), SC-35 (mouse; Sigma-Aldrich), coilin (rabbit, H-300; Santa Cruz Biotechnology, Inc.), Pol II pS2 (rabbit, ab5095; Abcam), Pol II pS5 (mouse, ab5408; Abcam), BrdU (mouse, B8434; Sigma-Aldrich), and Lamin A/C (mouse, ab40567; Abcam).

Live cell imaging

For live cell imaging of U2OS cells stably expressing EGFP-53BP1, cells were imaged with an ImageXpress Micro System (Molecular Devices) fitted with a 20 \times lens and equipped with a 37°C heating chamber supplied with CO₂. Images were acquired with MetaExpress software. U2OS cells stably expressing EGFP-53BP1 and mRuby-PCNA were plated on glass-bottomed dishes (WillCo) in Leibovitz's L15 medium (Invitrogen) containing 10% FBS, and images were acquired with a DeltaVision microscope (Applied Precision) equipped with a 37°C heating chamber, a 40 \times objective lens, and SoftWoRx software. Images were deconvolved after acquisition.

3D DNA immuno-FISH

DNA FISH on 3D preserved nuclei was performed by broadly following a published protocol (Cremer et al., 2008). In brief, BJ hTERT cells grown on glass coverslips were fixed for 10 min with 4% FA in PBS, permeabilized with 0.5% Triton X-100/PBS for 10 min at RT, and then incubated with RNase A (Sigma-Aldrich; 200 μ g/ml in PBS) for 1–2 h at 37°C. Human chromosomes 2, 3, 6, 7, 14, 16, and 17 were detected with directly labeled (green fluorophore) whole chromosome painting probes (Aquarius liquid format) obtained from Cytocell. Cellular DNA and the DNA FISH probes were denatured for 3 min, and hybridization was performed for 16–24 h at 37°C. Coverslips were washed at 37°C twice for 10 min each, with 50% formamide/2 \times saline-sodium citrate (SSC), 0.05% Tween-20/2 \times SSC, and 0.2 \times SSC. 53BP1 was then detected with a rabbit polyclonal antibody (Novus Biologicals) and Alexa Fluor 594-conjugated goat anti-rabbit antibody (Invitrogen).

ChIP-seq

In vivo cross-linking, chromatin purification, and immunoprecipitations were performed essentially as described previously (Orlando et al., 1997) with the following modifications. BJ hTERT fibroblasts were serum-starved (DME containing 0.5% FBS plus PSQF). Subsequently, cells were cross-linked for 15 min at RT. Nuclei were resuspended in sonication buffer (50 mM Tris, pH 8,

1% SDS, and 10 mM EDTA) and sonicated with a Bioruptor (Diagenode) at 30-s intervals. CHIP was performed with rabbit IgG (Santa Cruz Biotechnology, Inc.) or rabbit anti- γ H2AX (07-164; Millipore) and Protein G-Sepharose beads (Sigma-Aldrich). DNA was eluted in a buffer containing 1% SDS and 100 mM NaHCO₃. After RNase and Proteinase K treatment, DNA was purified with a QIAquick PCR purification kit (QIAGEN). Libraries for CHIP-seq were generated with a kit essentially as described by the manufacturer (Illumina, Inc.). Amplified DNA was run on 2% agarose gels and stained with SYBR green I (Invitrogen). Bands between 100 and 300 bp were excised, gel purified, and submitted to the Cambridge Research Institute (CRI) for sequencing. Resulting reads were mapped against the human genome (GRCh37) with bwa (Li and Durbin, 2009). Reads with bwa quality scores >13 were extended to the mean library length (200 bp). Resulting data were binned to 20-bp regions for display on the UCSC Genome Browser (Kent et al., 2002). Peaks were called using MACS 1.3.7 (Zhang et al., 2008) and HPeaks 1.1 (Qin et al., 2010) with IgG and γ H2AX as negative and positive controls, respectively. The intersection of overlapping peaks from both peak callers was used as a guide for visual inspection of the peaks. A final list of peaks was generated after the removal of false positives.

Flow cytometry

Cells were harvested by trypsinization, pelleted, resuspended in PBS, and fixed with cold 70% ethanol. The next day, cells were pelleted and resuspended in PBS containing 250 μ g/ml RNase A and 10 μ g/ml propidium iodide and incubated for 30 min at 37°C. Cells were analyzed with a FACSCalibur (Beckman Coulter) using CellQuest software.

Western immunoblotting

Cells were washed with PBS, scraped in Laemmli buffer (120 mM Tris, pH 6.8, 4% SDS, and 20% glycerol), boiled for 5 min at 95°C, and syringed. Lysates were loaded on a 3–8% Tris-Acetate (Fig. 6 E) or 4–12% Tris-Glycine (Fig. S2 B) gel (Invitrogen), and proteins were transferred onto a polyvinylidene fluoride membrane. The membrane was blocked with 5% nonfat milk in TBS-T and incubated with primary antibodies for 1 h at RT. After washes with TBS-T, the membrane was incubated with the corresponding horseradish peroxidase-conjugated secondary antibodies for 1 h at RT. Antigen-antibody complexes were detected by enhanced chemiluminescence by ECL (GE Healthcare). Antibodies used for Western blotting were: ATR (goat, N19; Santa Cruz Biotechnology, Inc.), FANCD2 (mouse, F17; Santa Cruz Biotechnology, Inc.), GRB2 (mouse; BD), or PARP-1 (rabbit, 9542; Cell Signaling Technology).

Online supplemental material

Fig. S1 shows that 53BP1 nuclear bodies do not colocalize with fibrillarin, coilin, or SC-35. Fig. S2 demonstrates that 53BP1-OPT domains form in ATR-deficient Seckel cells. Fig. S3 demonstrates that Oct-1 and PTF localize to sites of DNA damage formed by laser micro-irradiation. Fig. S4 shows an increase in the number of PTF δ and PML bodies that colocalize with 53BP1 after treatment of cells with a low dose of APH. Online supplemental material is available at <http://www.jcb.org/cgi/content/full/jcb.201011083/DC1>.

We thank members of the Jackson laboratory for helpful discussions, and Abderrahmane Kaidi and Jorrit Tjeertes for critical reading of the manuscript. We are grateful to the Cambridge Research Institute for sequencing services.

S.P. Jackson receives his salary from the University of Cambridge, supplemented by Cancer Research UK (CRUK). Research in the S.P. Jackson laboratory is funded by CRUK program grant C6/A1 1224 and the European Community (GENICA). Core infrastructure funding is provided by CRUK and the Wellcome Trust. J.A. Harrigan was supported by an EU Project Grant (LSHG-CT-2005-512113) and a CRUK project grant (C6/A1 1221). D.S. Dimitrova and the P. Fraser laboratory were supported by the Biotechnology and Biological Sciences Research Council.

Submitted: 15 November 2010

Accepted: 3 March 2011

References

- Ahel, D., Z. Horejsi, N. Wiechens, S.E. Polo, E. Garcia-Wilson, I. Ahel, H. Flynn, M. Skehel, S.C. West, S.P. Jackson, et al. 2009. Poly(ADP-ribose)-dependent regulation of DNA repair by the chromatin remodeling enzyme ALC1. *Science*. 325:1240–1243. doi:10.1126/science.1177321
- Bouwman, P., A. Aly, J.M. Escandell, M. Pieterse, J. Bartkova, H. van der Gulden, S. Hiddingh, M. Thanasoulas, A. Kulkarni, Q. Yang, et al. 2010. 53BP1 loss rescues BRCA1 deficiency and is associated with triple-negative and BRCA-mutated breast cancers. *Nat. Struct. Mol. Biol.* 17:688–695. doi:10.1038/nsmb.1831

- Branzei, D., and M. Foiani. 2010. Maintaining genome stability at the replication fork. *Nat. Rev. Mol. Cell Biol.* 11:208–219. doi:10.1038/nrm2852
- Bunting, S.F., E. Callén, N. Wong, H.T. Chen, F. Polato, A. Gunn, A. Bothmer, N. Feldhahn, O. Fernandez-Capetillo, L. Cao, et al. 2010. 53BP1 inhibits homologous recombination in Brca1-deficient cells by blocking resection of DNA breaks. *Cell*. 141:243–254. doi:10.1016/j.cell.2010.03.012
- Celeste, A., O. Fernandez-Capetillo, M.J. Kruhlak, D.R. Pilch, D.W. Staudt, A. Lee, R.F. Bonner, W.M. Bonner, and A. Nussenzweig. 2003. Histone H2AX phosphorylation is dispensable for the initial recognition of DNA breaks. *Nat. Cell Biol.* 5:675–679. doi:10.1038/ncb1004
- Chan, K.L., P.S. North, and I.D. Hickson. 2007. BLM is required for faithful chromosome segregation and its localization defines a class of ultrafine anaphase bridges. *EMBO J.* 26:3397–3409. doi:10.1038/sj.emboj.7601777
- Chan, K.L., T. Palmai-Pallag, S. Ying, and I.D. Hickson. 2009. Replication stress induces sister-chromatid bridging at fragile site loci in mitosis. *Nat. Cell Biol.* 11:753–760. doi:10.1038/ncb1882
- Chapman, J.R., and S.P. Jackson. 2008. Phospho-dependent interactions between NBS1 and MDC1 mediate chromatin retention of the MRN complex at sites of DNA damage. *EMBO Rep.* 9:795–801. doi:10.1038/embo.2008.103
- Ciccia, A., and S.J. Elledge. 2010. The DNA damage response: making it safe to play with knives. *Mol. Cell.* 40:179–204. doi:10.1016/j.molcel.2010.09.019
- Cremer, M., F. Grasser, C. Lanctôt, S. Müller, M. Neusser, R. Zinner, I. Solovei, and T. Cremer. 2008. Multicolor 3D fluorescence in situ hybridization for imaging interphase chromosomes. *Methods Mol. Biol.* 463:205–239. doi:10.1007/978-1-59745-406-3_15
- Doil, C., N. Mailand, S. Bekker-Jensen, P. Menard, D.H. Larsen, R. Pepperkok, J. Ellenberg, S. Panier, D. Durocher, J. Bartek, et al. 2009. RNF168 binds and amplifies ubiquitin conjugates on damaged chromosomes to allow accumulation of repair proteins. *Cell*. 136:435–446. doi:10.1016/j.cell.2008.12.041
- Difilippantonio, S., E. Gapud, N. Wong, C.Y. Huang, G. Mahowald, H.T. Chen, M.J. Kruhlak, E. Callen, F. Livak, M.C. Nussenzweig, et al. 2008. 53BP1 facilitates long-range DNA end-joining during V(D)J recombination. *Nature*. 456:529–533. doi:10.1038/nature07476
- Dimitrova, D.S. 2009. Visualization of DNA replication sites in mammalian nuclei. *Methods Mol. Biol.* 521:413–436.
- Dimitrova, N., Y.C. Chen, D.L. Spector, and T. de Lange. 2008. 53BP1 promotes non-homologous end joining of telomeres by increasing chromatin mobility. *Nature*. 456:524–528. doi:10.1038/nature07433
- Durkin, S.G., and T.W. Glover. 2007. Chromosome fragile sites. *Annu. Rev. Genet.* 41:169–192. doi:10.1146/annurev.genet.41.042007.165900
- Galanty, Y., R. Belotserkovskaya, J. Coates, S. Polo, K.M. Miller, and S.P. Jackson. 2009. Mammalian SUMO E3-ligases PIAS1 and PIAS4 promote responses to DNA double-strand breaks. *Nature*. 462:935–939. doi:10.1038/nature08657
- Glover, T.W., C. Berger, J. Coyle, and B. Echo. 1984. DNA polymerase alpha inhibition by aphidicolin induces gaps and breaks at common fragile sites in human chromosomes. *Hum. Genet.* 67:136–142. doi:10.1007/BF00272988
- Hickson, I., Y. Zhao, C.J. Richardson, S.J. Green, N.M. Martin, A.I. Orr, P.M. Reaper, S.P. Jackson, N.J. Curtin, and G.C. Smith. 2004. Identification and characterization of a novel and specific inhibitor of the ataxia-telangiectasia mutated kinase ATM. *Cancer Res.* 64:9152–9159. doi:10.1158/0008-5472.CAN-04-2727
- Howlett, N.G., T. Taniguchi, S.G. Durkin, A.D. D'Andrea, and T.W. Glover. 2005. The Fanconi anemia pathway is required for the DNA replication stress response and for the regulation of common fragile site stability. *Hum. Mol. Genet.* 14:693–701. doi:10.1093/hmg/ddi065
- Iacovoni, J.S., P. Caron, I. Lassadi, E. Nicolas, L. Massip, D. Trouche, and G. Legube. 2010. High-resolution profiling of gammaH2AX around DNA double strand breaks in the mammalian genome. *EMBO J.* 29:1446–1457. doi:10.1038/emboj.2010.38
- Kent, W.J., C.W. Sugnet, T.S. Furey, K.M. Roskin, T.H. Pringle, A.M. Zahler, and D. Haussler. 2002. The human genome browser at UCSC. *Genome Res.* 12:996–1006.
- Lempiäinen, H., and T.D. Halazonetis. 2009. Emerging common themes in regulation of PIKKs and PI3Ks. *EMBO J.* 28:3067–3073. doi:10.1038/emboj.2009.281
- Li, H., and R. Durbin. 2009. Fast and accurate short read alignment with Burrows-Wheeler transform. *Bioinformatics*. 25:1754–1760. doi:10.1093/bioinformatics/btp324
- Li, L., K. Roy, S. Katyal, X. Sun, S. Bléoo, and R. Godbout. 2006. Dynamic nature of cleavage bodies and their spatial relationship to DDX1 bodies, Cajal bodies, and gems. *Mol. Biol. Cell*. 17:1126–1140. doi:10.1091/mbc.E05-08-0768
- Li, L., E.A. Monckton, and R. Godbout. 2008. A role for DEAD box 1 at DNA double-strand breaks. *Mol. Cell Biol.* 28:6413–6425. doi:10.1128/MCB.01053-08
- Lovejoy, C.A., and D. Cortez. 2009. Common mechanisms of PIKK regulation. *DNA Repair (Amst.)*. 8:1004–1008. doi:10.1016/j.dnarep.2009.04.006
- Manis, J.P., J.C. Morales, Z. Xia, J.L. Kutok, F.W. Alt, and P.B. Carpenter. 2004. 53BP1 links DNA damage-response pathways to immunoglobulin heavy chain class-switch recombination. *Nat. Immunol.* 5:481–487. doi:10.1038/ni1067
- Morales, J.C., Z. Xia, T. Lu, M.B. Aldrich, B. Wang, C. Rosales, R.E. Kellems, W.N. Hittelman, S.J. Elledge, and P.B. Carpenter. 2003. Role for the BRCA1 C-terminal repeats (BRCT) protein 53BP1 in maintaining genomic stability. *J. Biol. Chem.* 278:14971–14977. doi:10.1074/jbc.M212484200
- Orlando, V., H. Strutt, and R. Paro. 1997. Analysis of chromatin structure by in vivo formaldehyde cross-linking. *Methods*. 11:205–214. doi:10.1006/meth.1996.0407
- Palm, W., and T. de Lange. 2008. How shelterin protects mammalian telomeres. *Annu. Rev. Genet.* 42:301–334. doi:10.1146/annurev.genet.41.110306.130350
- Pombo, A., P. Cuello, W. Schul, J.B. Yoon, R.G. Roeder, P.R. Cook, and S. Murphy. 1998. Regional and temporal specialization in the nucleus: a transcriptionally-active nuclear domain rich in PTF, Oct1 and PIKA antigens associates with specific chromosomes early in the cell cycle. *EMBO J.* 17:1768–1778. doi:10.1093/emboj/17.6.1768
- Qin, Z.S., J. Yu, J. Shen, C.A. Maher, M. Hu, S. Kalyana-Sundaram, J. Yu, and A.M. Chinnaiyan. 2010. HPeak: an HMM-based algorithm for defining read-enriched regions in ChIP-Seq data. *BMC Bioinformatics*. 11:369. doi:10.1186/1471-2105-11-369
- Rai, R., H. Zheng, H. He, Y. Luo, A. Multani, P.B. Carpenter, and S. Chang. 2010. The function of classical and alternative non-homologous end-joining pathways in the fusion of dysfunctional telomeres. *EMBO J.* 29:2598–2610. doi:10.1038/emboj.2010.142
- Reina-San-Martin, B., J. Chen, A. Nussenzweig, and M.C. Nussenzweig. 2007. Enhanced intra-switch region recombination during immunoglobulin class switch recombination in 53BP1-/- B cells. *Eur. J. Immunol.* 37:235–239. doi:10.1002/eji.200636789
- Robertson, G., M. Hirst, M. Bainbridge, M. Bilenky, Y. Zhao, T. Zeng, G. Euskirchen, B. Bernier, R. Varhol, A. Delaney, et al. 2007. Genome-wide profiles of STAT1 DNA association using chromatin immunoprecipitation and massively parallel sequencing. *Nat. Methods*. 4:651–657. doi:10.1038/nmeth1068
- Salic, A., and T.J. Mitchison. 2008. A chemical method for fast and sensitive detection of DNA synthesis in vivo. *Proc. Natl. Acad. Sci. USA*. 105:2415–2420. doi:10.1073/pnas.0712168105
- Sartori, A.A., C. Lukas, J. Coates, M. Mistrik, S. Fu, J. Bartek, R. Baer, J. Lukas, and S.P. Jackson. 2007. Human CtIP promotes DNA end resection. *Nature*. 450:509–514. doi:10.1038/nature06337
- Schultz, L.B., N.H. Chehab, A. Malikzay, and T.D. Halazonetis. 2000. p53 binding protein 1 (53BP1) is an early participant in the cellular response to DNA double-strand breaks. *J. Cell Biol.* 151:1381–1390. doi:10.1083/jcb.151.7.1381
- Schwartz, M., E. Zlotorynski, and B. Kerem. 2006. The molecular basis of common and rare fragile sites. *Cancer Lett.* 232:13–26. doi:10.1016/j.canlet.2005.07.039
- Shanbhag, N.M., I.U. Rafalska-Metcalf, C. Balane-Bolivar, S.M. Janicki, and R.A. Greenberg. 2010. ATM-dependent chromatin changes silence transcription in cis to DNA double-strand breaks. *Cell*. 141:970–981. doi:10.1016/j.cell.2010.04.038
- Spector, D.L. 2006. SnapShot: Cellular bodies. *Cell*. 127:1071. doi:10.1016/j.cell.2006.11.026
- Stucki, M., and S.P. Jackson. 2006. gammaH2AX and MDC1: anchoring the DNA-damage-response machinery to broken chromosomes. *DNA Repair (Amst.)*. 5:534–543. doi:10.1016/j.dnarep.2006.01.012
- Ward, I.M., K. Minn, J. van Deursen, and J. Chen. 2003. p53 Binding protein 53BP1 is required for DNA damage responses and tumor suppression in mice. *Mol. Cell Biol.* 23:2556–2563. doi:10.1128/MCB.23.7.2556-2563.2003
- Ward, I.M., B. Reina-San-Martin, A. Orlano, K. Minn, K. Tamada, J.S. Lau, M. Cascalho, L. Chen, A. Nussenzweig, F. Livak, et al. 2004. 53BP1 is required for class switch recombination. *J. Cell Biol.* 165:459–464. doi:10.1083/jcb.200403021
- Zhang, Y., T. Liu, C.A. Meyer, J. Eeckhoutte, D.S. Johnson, B.E. Bernstein, C. Nusbaum, R.M. Myers, M. Brown, W. Li, and X.S. Liu. 2008. Model-based analysis of ChIP-Seq (MACS). *Genome Biol.* 9:R137. doi:10.1186/gb-2008-9-9-r137
- Zwilling, S., A. Annweiler, and T. Wirth. 1994. The POU domains of the Oct1 and Oct2 transcription factors mediate specific interaction with TBP. *Nucleic Acids Res.* 22:1655–1662. doi:10.1093/nar/22.9.1655